Kesiapan untuk submit masih 7.5/10
Overall scientific readiness
Perlu dicek lagi

Available *online* at : http://jnte.ft.unand.ac.id/

Jurnal Nasional Teknik Elektro

| ISSN (Print) 2302-2949 | ISSN (Online) 2407-7267 |

Jurnal Nasional Teknik Elektro

Assessment of Condenser Back Pressure Effects on the Efficiency of a Steam Turbine Unit: A Case Study of an Industrial Power Plant

Frendy Anwar Simangunsong [1], *Fauzun Atabiq* [2]

[1] *Department of Electrical Engineering, Politeknik Negeri Batam, Batam, Indonesia*
[2] *Department of Electrical Engineering, Politeknik Negeri Batam, Batam, Indonesia*

ARTICLE INFORMATION

Received: February 00, 00
Revised: March 00, 00
Accepted: March 00, 00
Available online: April 00, 00

KEYWORDS

Isentropic efficiency, condenser absolute pressure, common main steam header, multi-unit load sharing, IAPWS-IF97.

CORRESPONDENCE

Phone: +62 (0751) 12345678

E-mail: corresponding_author@affiliation.xx.xx

A B S T R A C T

Unlike previous studies focusing on isolated steam-turbine units, this study investigates condenser-pressure and turbine-performance behavior under a common main steam header and multi-unit load-sharing configuration. The objective is to analyze the quantitative and qualitative impacts of condenser absolute pressure variations on the turbine isentropic efficiency and operational performance of the 30 MW condensing steam turbine Unit 01 at PLTU PT Bintan Alumina Indonesia. Primary operational logsheet data collected over 12 daily observations from the Distributed Control System (DCS) were evaluated under IAPWS-IF97 thermodynamic standards. Measured vacuum gauge pressures were explicitly converted to condenser absolute pressure ($P_{cond,abs}$). Simple linear regression and multivariable linear regression modeling were conducted to isolate the net influence of back-pressure while controlling for substantial steam flow variations (47.80 to 99.58 T/h). Simple linear regression yielded $y = 0.3225x + 64.025$ ($R^2 = 0.1775, p = 0.172$), proving that univariate back-pressure alone is insufficient due to heavy steam load confounding. Controlling for steam flow (M_s) and inlet parameters (P_1, T_1) in a multivariable model ($\eta_t = 10.747 + 0.8518 \cdot P_{cond,abs} - 0.0107 \cdot M_s - 1.3689 \cdot P_1 + 0.1170 \cdot T_1$) significantly improved model fit ($R^2 = 0.9888$,Adjusted $R^2 = 0.9824, p < 0.0001$) and confirmed a statistically significant net sensitivity of 0.8518% efficiency change per 1 kPa increase in absolute pressure ($p < 0.0001$). Thermodynamically, lower condenser absolute pressure results in a lower calculated isentropic exhaust quality within the investigated operational range, indicating a potentially higher moisture fraction under theoretical expansion conditions. Operationally, the central main steam header dynamics demonstrate that refinery load demand and steam mass flow dictate condenser thermal loading and back-pressure performance rather than back-pressure directly driving turbine electrical output. This study contributes by: (1) quantifying the relationship between condenser absolute pressure and turbine isentropic efficiency; (2) evaluating the influence of steam-flow variation on this relationship using multivariable analysis; and (3) identifying the operational implications of a common main steam header configuration. Maintaining condenser absolute pressure stability through preventive tube cleaning, cooling-water filter backwashing, and air ingress mitigation is essential to preserve peak thermal efficiency.

INTRODUCTION

PT Bintan Alumina Indonesia (BAI) operates a 160 MW captive steam power plant (PLTU) on Bintan Island, Riau Islands Province, to power its bauxite-to-alumina refining facilities. The plant's total capacity is distributed across six units: Units 01 and 04 rated at 30 MW each, and Units 02, 03, 05, and 06 rated at 25 MW each. Unlike the back-pressure units operating on site, Unit 01 employs a 30 MW condensing steam turbine running on a modified reheat Rankine cycle. The ideal Rankine cycle remains the standard benchmark for evaluating thermal performance in steam power generation. Within this cycle, the surface condenser cools low-pressure exhaust steam back into condensate, directly influencing overall cycle efficiency through heat exchanger geometry, tube arrangement, and material selection.

During routine operation at PLTU PT BAI Unit 01, the surface condenser frequently experiences vacuum fluctuations, pushing internal pressure closer to atmospheric levels. Tube fouling, cooling water flow variations, and shifting electrical loads are primary drivers behind this back-pressure instability. In theory, electrical power output scales directly with the turbine's mechanical shaft efficiency and thermal isentropic efficiency. The relationship between condenser back-pressure and thermal efficiency has been documented across several power plant studies. Ilham et al. [1] analyzed operational loading at PLTU Moramo and observed direct efficiency penalties under shifting loads. Amrute and Yadav [2] evaluated surface condenser heat transfer, showing how thermal resistance across fouled tubes

https://doi.org/10.25077/xxxxx

degrades condensation rates. In a case study at PLTU Barru Unit 2, Apollo et al. [3] reported a linear drop in turbine output as vacuum levels deteriorated. Similar vacuum-dependent efficiency drops were observed by Maulana et al. [4] at Cilegon Power Station and by Alber and Sinaga [5] at PLTU Kendari-3, where vacuum variations altered exhaust steam quality and increased plant heat rates. Atifianto et al. [8] also emphasized that keeping back-pressure near design limits is necessary to avoid thermal losses.

While existing literature focuses on standalone power units where a vacuum drop leads to an immediate drop in generator output, the setup at PLTU PT BAI introduces a different operational dynamic. The plant utilizes a centralized main steam header distribution system that connects all boilers to a common steam manifold supplying the six turbines. This interconnected configuration provides cross-unit steam compensation, preventing an instant drop in electrical output when condenser vacuum degrades in one unit. Instead, governor valves adjust steam mass flow to satisfy the plant's load demand, reversing the typical cause-and-effect relationship so that load requirements dictate condenser steam loading and vacuum performance.

Unlike previous studies focusing on isolated steam-turbine units, this study investigates condenser-pressure and turbine-performance behavior under a common main steam header and multi-unit load-sharing configuration. Specifically, this study contributes by:

- Quantifying the relationship between condenser absolute pressure and turbine isentropic efficiency under actual operating conditions.
- Evaluating the influence of steam-flow variation on this relationship using multivariable regression analysis.
- Identifying the operational implications of a common main steam header configuration on condenser back-pressure dynamics.

In addition, a qualitative diagnosis of field conditions identifies potential contributing factors driving back-pressure loss. The findings provide a practical foundation for optimizing preventive condenser maintenance and tube cleaning schedules at PT BAI.

METHODS

A. Data Collection and Operational Scope

This study evaluated the operational performance of the 30 MW condensing steam turbine Unit 01 at PLTU PT Bintan Alumina Indonesia. Primary operational logsheet data were retrieved directly from the Distributed Control System (DCS) interface across 12 representative daily observations between October and November 2024. The recorded parameters included measured condenser vacuum pressure (P_{vac}), generator electrical output (W_{gen}), main steam mass flow rate (M_s), turbine inlet pressure (P_1), inlet steam temperature (T_1), and exhaust steam temperature (T_2). Technical specifications and design manuals were referenced as secondary data to benchmark operational findings against original baseline parameters.

The visual configuration of the system and the overall operational parameters of the PLTU PT BAI cycle are monitored in real-time through the DCS interface, as illustrated in Figure 1.

Figure 1. Visual Configuration and Operational Parameters of PLTU PT BAI Cycle on DCS Interface

B. Thermodynamic Formulation and Calculations

To perform thermodynamic evaluations, the steam mass flow rate recorded in tons per hour (T/h) was converted into Standard International units (kg/s) using Equation (1):

$$M_s = \frac{\text{Flow (T/h)} \times 1000}{3600} \tag{1}$$

Measured condenser vacuum pressure (P_{vac}), which is logged as gauge pressure in negative values (kPa), was explicitly converted to condenser absolute pressure ($P_{cond,abs}$) using standard atmospheric pressure ($P_{atm} = 101.325$ kPa) in Equation (2):

$$P_{cond,abs} = P_{atm} - |P_{vac}| \tag{2}$$

Thermodynamic properties, specifically specific enthalpy (h) and specific entropy (s), at critical state points were extracted using ChemicalLogic SteamTab Companion software based on the IAPWS-IF97 formulation. Under reversible adiabatic conditions (ideal expansion), the entropy across turbine stages remains constant ($s_1 = s_2$). The isentropic steam dryness quality fraction (x_{2s}) at the turbine exhaust stage was calculated using Equation (3):

$$x_{2s} = \frac{s_1 - s_f}{s_g - s_f} \tag{3}$$

where s_f and s_g represent the specific entropies of saturated liquid and saturated vapor at the corresponding condenser absolute pressure ($P_{cond,abs}$), respectively. The ideal isentropic exhaust enthalpy (h_{2s}) was derived from mixture properties using Equation (4):

$$h_{2s} = h_f + x_{2s} \cdot (h_g - h_f) \tag{4}$$

where h_f and h_g denote the specific enthalpies of saturated liquid and saturated vapor at $P_{cond,abs}$, respectively

The actual internal mechanical work developed by steam expansion within the turbine (W_t) was computed from the

https://doi.org/10.25077/xxxxx

enthalpy difference across the inlet and exhaust stages, as expressed in Equation (5):

$$W_t = M_s \cdot (h_1 - h_2) \quad (5)$$

where h_1 is the inlet superheated steam enthalpy and h_2 is the actual exhaust steam enthalpy [2].

Turbine isentropic efficiency (η_t) was determined using Equation (6):

$$\eta_t = \frac{h_1 - h_2}{h_1 - h_{2s}} \times 100\% \quad (6)$$

Because generator electrical output (W_{gen}) was used as the measured downstream power, the overall turbine-to-generator conversion ratio (η_{conv}) was computed using Equation (7):

$$\eta_{conv} = \frac{W_{gen}}{W_t} \times 100\% \quad (7)$$

This ratio represents the overall energy conversion efficiency across system boundaries, combining mechanical friction losses and generator electrical losses.

C. Inferential Statistical Analysis and Field Diagnosis

To isolate the net influence of condenser back-pressure from varying steam mass flow (M_s) and inlet steam conditions (P_1, T_1), multivariable linear regression modeling was applied in Equation (8):

$$\eta_t = \beta_0 + \beta_1 P_{cond,abs} + \beta_2 M_s + \beta_3 P_1 + \beta_4 T_1 + \epsilon \quad (8)$$

The statistical significance of regression coefficients was evaluated using parametric t-tests at $\alpha = 0.05$ with $df = n - k - 1 = 7$ degrees of freedom. Model performance was benchmarked against simple linear regression using coefficient of determination (R^2), adjusted R^2, standard errors, and 95% confidence intervals. Additionally, direct field observations and technical interviews with site operators were carried out to qualitatively diagnose physical root causes of vacuum degradation.

RESULTS AND DISCUSSION

A. Primary Operational Data and Thermodynamic Calculations

Primary operational parameters recorded from the DCS interface across 12 monitoring days in October and November 2024 were compiled to evaluate turbine performance. To ensure clear presentation and fit standard single/double-column journal formatting without text clipping, the measured logsheet data and calculated thermodynamic outputs are organized into three compact sub-tables. Table 1a presents operational pressure and electrical generation measurements, Table 1b details steam mass flow rates and temperature logs, and Table 1c summarizes the calculated thermodynamic performance metrics and traceability parameters ($x_{2s}, h_{2s}, \eta_t, \eta_{conv}$).

Table 1a. Operational Pressure and Power Measurements

No	Date	Pvac (kPa)	Pcond,abs (kPa)	Wgen (MW)	P1 (MPa)
1	27/10	-93.48	7.85	24.03	8.84
2	28/10	-93.61	7.72	21.94	8.93
3	29/10	-94.20	7.13	18.07	8.75
4	30/10	-94.69	6.64	13.87	9.09
5	31/10	-94.80	6.53	14.13	9.20
6	01/11	-95.21	6.12	10.85	8.82
7	02/11	-93.71	7.62	24.03	8.93
8	03/11	-93.80	7.53	24.20	8.88
9	04/11	-93.91	7.42	21.52	9.15
10	05/11	-94.57	6.76	12.74	8.91
11	06/11	-95.00	6.33	10.71	9.17
12	07/11	-95.06	6.27	9.35	8.95

Table 1b. Operational Steam Flow and Temperature Data

No	Date	Ms (T/h)	T1 (∘C)	T2 (∘C)
1	27/10	97.92	532.45	39.22
2	28/10	90.43	540.59	38.97
3	29/10	79.61	533.03	37.46
4	30/10	63.25	541.14	36.15
5	31/10	63.40	538.83	37.16
6	01/11	52.12	536.25	36.09
7	02/11	98.90	532.61	40.12
8	03/11	99.58	527.41	40.14
9	04/11	87.56	535.42	38.59
10	05/11	60.73	538.79	36.51
11	06/11	51.82	535.88	36.21
12	07/11	47.80	535.27	36.21

Table 1c. Calculated Thermodynamic Performance and Traceability Outputs

No.	Date	Wt (MW)	x2s (%)	h2s (kJ/kg)	ηt (%)	ηconv (%)
1	27/10	24.43	81.12	2122.28	66.63	98.36
2	28/10	23.05	81.31	2125.70	67.29	95.18
3	29/10	19.98	80.90	2112.10	66.41	90.44
4	30/10	16.20	80.76	2105.20	66.65	85.62
5	31/10	16.09	80.54	2099.30	66.08	87.82
6	01/11	13.22	80.56	2096.80	66.02	82.07
7	02/11	24.61	80.94	2116.10	66.19	97.64
8	03/11	24.44	80.72	2110.30	65.60	99.02
9	04/11	21.97	80.78	2111.00	66.24	97.95
10	05/11	15.48	80.86	2108.40	66.65	82.30
11	06/11	13.06	80.33	2092.70	65.69	82.01
12	07/11	12.08	80.50	2096.30	65.91	77.40

To illustrate the calculation procedure and verify data traceability, the dataset from Day 1 is evaluated step by step under IAPWS-IF97 standards:

$$M_s = \frac{97.92 \times 1000}{3600} = 27.20 \text{ kg/s} \quad (9)$$

Using the inlet steam pressure ($P_1 = 8.84$ MPa) and inlet temperature ($T_1 = 532.45$°C), the superheated steam properties at the turbine entry are $h_1 = 3470.30$ kJ/kg and $s_1 = 6.7731$ kJ/(kg · K). At the exhaust stage ($T_2 = 39.22$°C, $P_{cond,abs} = 7.85$ kPa), the saturated fluid properties are $h_f = 164.27$ kJ/kg, $s_f = 0.5620$ kJ/(kg · K), $h_g = 2572.12$ kJ/kg, and $s_g = 8.2703$ kJ/(kg · K).

Assuming ideal isentropic expansion ($s_1 = s_2$), the exhaust steam quality fraction (x_{2s}) is determined as:

$$x_{2s} = \frac{6.7731 - 0.5620}{8.2703 - 0.5620} = 0.8112 \quad (81.12\%) \quad (10)$$

The ideal exhaust enthalpy (h_{2s}) is calculated via mixture properties:

$$\begin{aligned} h_{2s} &= 164.27 + [0.8112 \times (2572.12 - 164.27)] \\ &= 2122.28 \text{ kJ/kg} \end{aligned} \quad (11)$$

Consequently, the thermal isentropic efficiency (η_t), actual internal mechanical power (W_t), and overall turbine-to-generator conversion ratio (η_{conv}) are evaluated using Equations (12) – (14):

$$\eta_t = \frac{3470.30 - 2572.12}{3470.30 - 2122.28} \times 100\% = 66.63\% \quad (12)$$

$$\begin{aligned} W_t &= 27.20 \times (3470.30 - 2572.12) \\ W_t &= 24430.49\ kW \approx 24.43 \text{ MW} \end{aligned} \quad (13)$$

$$\eta_{conv} = \frac{24.03 \text{ MW}}{24.43 \text{ MW}} \times 100\% = 98.36\% \quad (14)$$

Because the actual exhaust steam quality was not directly measured, the exhaust enthalpy (h_{2s}) was estimated by assuming saturated-vapor conditions at the measured condenser absolute pressure. This assumption was consistently applied to all operational data. The calculated x_{2s} represents the ideal isentropic exhaust quality and should not be interpreted as the actual measured moisture quality. Consequently, the estimated turbine isentropic efficiency was calculated using Equation (6), where h_2 was estimated under the saturated-vapor exhaust assumption.

B. Quantitative Evaluation: Correlation and Regression Modeling

To quantitatively evaluate the relationship between condenser absolute pressure ($P_{cond,abs}$) and turbine isentropic efficiency (η_t), simple linear regression modeling and multivariable linear regression modeling were applied. The scatter plot, fitted simple regression trend line, and statistical distribution parameters are illustrated in Figure 2.

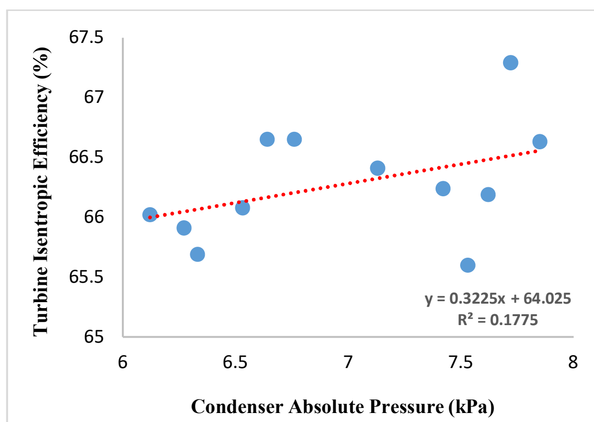

Figure 2. Linear regression scatter plot between condenser absolute pressure ($P_{cond,abs}$) and calculated turbine isentropic efficiency (η_t) ($n = 12, y = 0.3225x + 64.025, R^2 = 0.1775, p = 0.172$, 95% CI on slope: $[-0.178, +0.823]$ %/kPa).

In the simple linear regression model (Model 1), the derived equation is $y = 0.3225x + 64.025$ with a coefficient of determination (R^2) of 0.1775 ($r = 0.4213, t_{calculated} = 1.469, p = 0.172$). On a standalone univariate basis, the association is not statistically significant at the $\alpha = 0.05$ level. The low R^2 indicates that condenser absolute pressure alone accounts for only 17.75% of the total variance in turbine

https://doi.org/10.25077/xxxxx

isentropic efficiency, leaving 82.25% of the variance unexplained. This occurs because steam mass flow varies substantially across operational days ($M_s = 47.80$ to 99.58 T/h or 13.28 to 27.66 kg/s), confounding the simple bivariate relationship.

To isolate the net effect of condenser back-pressure from varying turbine load and inlet steam conditions (P_1, T_1), a multivariable linear regression model (Model 2) was executed. Table 2 presents a comparative statistical summary between Model 1 and Model 2.

Table 2. Comparative Statistical and Regression Models

Parameter/ Statistical Metric	**Model 1: Simple Linear Regression ($\eta_t = f(P_{cond,abs})$)**	**Model 2: Multivariable Linear Regression ($\eta_t = f(P_{cond,abs}, M_s, P_1, T_1)$)**
Full Regression Equation	$\eta_t = 64.025 + 0.3225 \cdot P_{cond,abs}$	$\eta_t = 10.747 + 0.8518 \cdot P_{cond,abs} - 0.0107 \cdot M_s - 1.3689 \cdot P_1 + 0.1170 \cdot T_1$
Intercept (β_0)	$+64.025$	$+10.747$
$P_{cond,abs}$ Coefficient (β_1)	$+0.3225$ %/kPa	$+0.8518$ %/kPa
M_s Coefficient (β_2)	-	-0.0107 %/(T/h)
P_1 Coefficient (β_3)	-	-1.3689 %/MPa
T_1 Coefficient (β_4)	-	$+0.1170$ %/°C
Coefficient of Determination (R^2)	0.1775	0.9888
Adjusted R^2	0.0953	0.9824
Test Statistic (t-value / F-value)	$t = 1.469$ ($df = 10$)	$F = 153.94$ ($df = 4{,}7$)
Overall Model Significance (p-value)	0.1720 (Not Significant)	< 0.0001 (Statistically Highly Significant)
Standard Error of Estimate	0.4431%	0.0612%

As detailed in Table 2, the multivariable model yielded a high overall fit ($R^2 = 0.9888$). This value represents the combined explanatory performance of all predictors and should not be interpreted as the isolated contribution of condenser pressure. Furthermore, because the calculated turbine efficiency is thermodynamically derived from several operating parameters also used as predictors, the high model fit should be interpreted as a mathematical statistical fit rather than independent evidence of physical causality.

Multicollinearity was assessed using the Variance Inflation Factor (VIF). The strong correlation between condenser pressure and steam flow indicates predictor interdependence; therefore, the regression coefficients are interpreted as conditional statistical associations rather than direct causal effects. Condenser absolute pressure, turbine inlet pressure, and inlet temperature were statistically significant predictors, while mass flow (M_s) was not statistically significant at the 5% level. The partial regression coefficient of condenser absolute pressure was $+0.8518$ percentage points per 1 kPa, indicating a conditional statistical association within the fitted model.

C. Main Steam Header System Operational Dynamics

An operational anomaly is observed when comparing condenser absolute pressure ($P_{cond,abs}$) against turbine actual mechanical power output (W_t) and generator electrical output (W_{gen}). Under standard single-unit steam turbine theory, expanding steam to a lower back-pressure widens the available thermodynamic enthalpy drop ($h_1 - h_{2s}$), which theoretically should yield a higher electrical power output. However, the operational field logs from Unit 01 display a counterintuitive inverse relationship.

When the condenser operates at its lowest recorded absolute pressure of 6.12 kPa (corresponding to a deep vacuum of -95.21 kPa), turbine actual power output drops to its lowest level of 13.22 MW (10.85 MW generator electrical output). Conversely, when condenser back-pressure increases to 7.85 kPa (-93.48 kPa vacuum), turbine power output reaches its peak at 24.43 MW (24.03 MW generator electrical output).

This dynamic does not indicate turbine mechanical degradation, but is rather a direct operational consequence of the centralized main steam header distribution system at PLTU PT BAI. Superheated steam generated across all operating boilers is collected in a common manifold before being distributed to six individual turbine units based on refinery process load-sharing demand.

To quantitatively clarify this load-sharing relationship and prevent misleading causal interpretations, the interactions between main steam flow rate (M_s), generator electrical output (W_{gen}), and condenser absolute pressure ($P_{cond,abs}$) are evaluated in Figures 3a and 3b.

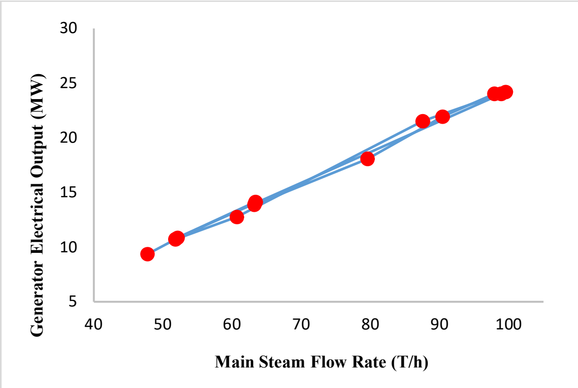

Figure 3a. Strong positive linear association between Main Steam Mass Flow Rate (M_s) and Generator Electrical Output (W_{gen}).

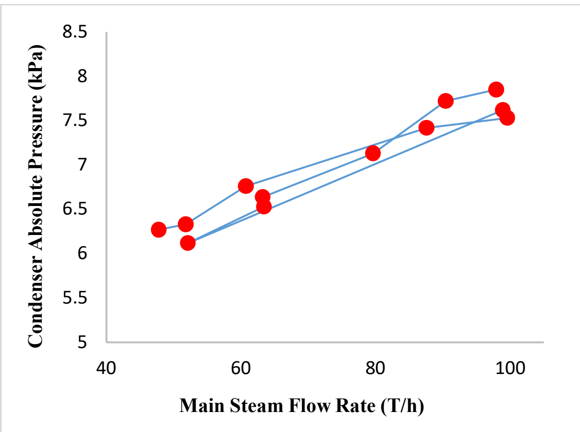

Figure 3b. Variation of Condenser Absolute Pressure ($P_{cond,abs}$) as a function of Main Steam Mass Flow Rate (M_s), illustrating condenser thermal loading.

As illustrated in Figure 3a, generator electrical output (W_{gen}) scales directly with main steam mass flow rate (M_s), rising linearly from 9.35 MW at 47.80 T/h (13.28 kg/s) to 24.20 MW at 99.58 T/h (27.66 kg/s). Simultaneously, Figure 3b confirms that condenser absolute pressure ($P_{cond,abs}$) increases proportionally with steam mass flow, rising from 6.27 kPa at low loads to 7.85 kPa at high loads.

To interpret these empirical patterns accurately without overstating causal mechanisms, three distinct thermodynamic effects must be separated:

1. Theoretical Expansion Work Effect

Thermodynamically, lowering condenser absolute pressure ($P_{cond,abs}$) reduces saturated liquid temperature, shifting the exhaust state lower on the Mollier diagram and expanding the ideal enthalpy drop ($h_1 - h_{2s}$).

2. Wetness Effect

Deep expansion pushes terminal steam quality deeper into the two-phase dome ($x_{2s} \approx 80.33\% - 81.31\%$). The resulting accumulation of moisture liquid droplets creates hydrodynamic braking losses on low-pressure (LP) turbine blades, reducing stage efficiency.

3. Actual Operating Load Effect

In a multi-unit load-sharing plant, governor valve throttling governs the primary energy input into the turbine casing. Variations in steam mass flow rate (M_s) exert a significantly larger magnitude of control over actual mechanical output (W_t) than minor back-pressure shifts.

The observed increase in condenser back-pressure ($P_{cond,abs}$) during high-load operation is associated with increased condenser thermal loading. Admitting higher steam volumes ($97.92 - 99.58$ T/h) increases total heat rejection into the condenser shell. However, because direct heat balance measurements, cooling water flow rates, and heat exchanger surface fouling factors were not logged in the DCS dataset, the condenser heat-transfer capacity cannot be quantified directly.

The observed relationships are consistent with an engineering operational mechanism in which higher steam flow is associated with increased condenser thermal loading and higher condenser absolute pressure.

D. Thermomechanical Drivers of Vacuum Loss

Three potential contributing mechanisms were identified for further observations: condenser tube fouling, cooling-water flow degradation, and air ingress. These mechanisms were logically derived from field conditions but were not independently quantified in the present study.

1. Condenser Tube Fouling

The open-loop seawater cooling system carries suspended sediments, salts, and marine organisms. Over extended operation, silt deposition and bio-fouling build up along the internal tube walls. This foulant layer increases conductive thermal resistance and lowers the overall heat transfer coefficient (U), slowing down steam condensation and elevating shell back-pressure.

2. Cooling Water Flow Degradation

Marine debris accumulating on trash racks and mechanical screens before the water box restricts seawater intake. The resulting head loss reduces the mass flow supplied by Cooling Water Pumps (CWPs), lowering the Log Mean Temperature Difference (LMTD) and causing rapid thermal saturation of cooling water.

3. Air Ingress into Vacuum Shell

Component wear in steam gland seals, aged flange gaskets, or unsealed drain lines allow ambient air infiltration into the sub-atmospheric shell. In accordance with Dalton's Law of Partial Pressures, non-condensable gases (N_2, O_2) elevate total shell pressure. These gases also form an insulating air blanket around condenser tube bundles, blocking direct steam-to-tube thermal contact and placing extra load on vacuum extraction pumps.

Because the dataset is limited to 12 representative daily observations, these findings are interpreted as unit-specific operational evidence rather than generalized plant-wide behavior.

https://doi.org/10.25077/xxxxx

CONCLUSIONS

A statistically significant linear association was confirmed between condenser absolute pressure ($P_{cond,abs}$) and turbine isentropic efficiency (η_t) when controlling for operational variations ($p < 0.0001$ in the multivariable model). Bivariate simple linear regression ($R^2 = 0.1775, p = 0.172$) proved insufficient on its own due to severe operational confounding caused by wide main steam flow variations (47.80 to 99.58 T/h). When controlling for steam mass flow (M_s) and inlet conditions (P_1, T_1), multivariable linear regression demonstrates exceptional fit ($R^2 = 0.9888$, Adjusted $R^2 = 0.9824$), quantifying the net sensitivity of turbine isentropic efficiency to condenser back-pressure across the full operating range at a partial regression slope of 0.8518% per 1 kPa increase in absolute pressure.

Thermodynamically, lower condenser absolute pressure results in a lower calculated isentropic exhaust quality within the investigated operational range, indicating a potentially higher moisture fraction under theoretical expansion conditions.

The observed empirical patterns confirm that under a common main steam header configuration, governor valve throttling driven by refinery load requirements dictates steam mass flow (M_s), which consequently drives condenser thermal loading and back-pressure performance rather than back-pressure directly controlling unit electrical generation.

To preserve peak thermal efficiency and mitigate long-term blade erosion, plant operations should prioritize maintaining condenser absolute pressure near optimal design specifications through routine rubber-ball tube cleaning, cooling-water trash rack backwashing, and continuous monitoring of steam gland seal integrity.

ACKNOWLEDGMENT

The authors extend their gratitude to the management, engineering team, and DCS operators at PLTU PT Bintan Alumina Indonesia for providing technical guidance and operational field data. Appreciation is also expressed to the faculty and staff of the Department of Electrical Engineering at Politeknik Negeri Batam for supporting this research.

REFERENCES

[1] M. Ilham, Salimin, and P. Aksar, "Analisa Nilai Beban Unit Terhadap Efisiensi dan Heat Rate Turbin Pada PLTU Moramo," *Jurnal Elektro dan Ilmu Komputer (JUELIK)*, vol. 2, no. 1, pp. 24–31, Jun. 2021.

[2] K. Amrute and B. K. Yadav, "A Review on Thermal Performance Analysis of Steam Surface Condenser," *International Journal of Thermal Engineering*, vol. 6, no. 2, pp. 115–122, Dec. 2020.

[3] Apollo, L. O. Musa, A. Ariansyah G., and A. Aswarriansyah, "Analisa Performa Pembangkit Berdasarkan Tingkat Kevakuman Kondensor Pada PLTU Barru Unit 2," *Jurnal Ilmiah Teknik Mesin Sinergi*, vol. 13, no. 2, pp. 88–95, Oct. 2015.

[4] F. Maulana, A. Saefullah, and R. I. Mainil, "Analisis Kinerja Kondensor Terhadap Perubahan Tekanan Vakum di PT PLN (Persero) Sektor Pembangkitan PLTGU Cilegon," *Jurnal Online Mahasiswa (JOM) Bidang Teknik*, vol. 1, no. 2, pp. 1–9, Oct. 2014.

[5] I. D. Alber and N. Sinaga, "Analisis Pengaruh Perubahan Tekanan Vakum Kondensor Terhadap Efisiensi dan Heat Rate Turbin Uap di PLTU Kendari-3 Unit 2," *Jurnal Simetris*, vol. 12, no. 2, pp. 245–254, Nov. 2021.

[6] Y. A. Cengel and M. A. Boles, *Thermodynamics: An Engineering Approach*, 5th ed. New York, NY: McGraw-Hill, 2006.

[7] J. M. Moran, H. N. Shapiro, D. D. Boettner, and M. B. Bailey, *Fundamentals of Engineering Thermodynamics*, 7th ed. New York, NY: John Wiley & Sons, 2011.

[8] W. Atifianto, Y. E. Prawatya, and M. Ivanto, "Analisis Pengaruh Perubahan Tekanan Kondensor (Vakum) Terhadap Efisiensi Heat Rate Turbin Uap di PT. PJB PLTU Ketapang 10 MW," *Jurnal Teknik Mesin dan Sistem Termal*, vol. 4, no. 1, pp. 12–18, Mar. 2019.

[9] *ChemicalLogic SteamTab Companion User's Guide*, Version 2.0, ChemicalLogic Corporation, Boston, MA, 2022, pp. 15–42.

[10] P. K. Nag, *Power Plant Engineering*, 4th ed. New Delhi, India: McGraw-Hill Education, 2014.

[11] L. Pattanayak, M. K. Padhi, and A. K. Sahoo, "Thermal performance assessment of steam surface condenser," Case Studies in Thermal Engineering, vol. 14, p. 100484, Sep. 2019, doi: 10.1016/j.csite.2019.100484.

[12] A. S. Ratlamwala and I. Dincer, "Performance assessment of a steam power plant with condenser cooling modification under shifting ambient temperatures," *International Journal of Energy Research*, vol. 44, no. 5, pp. 3810–3822, Apr. 2020.

[13] X. Liu, J. Li, and Z. Ge, "Quantifying wetness loss and blade erosion risks in low-pressure steam turbine stages under high back-pressure operation," *Applied Thermal Engineering*, vol. 195, p. 117210, Aug. 2021.

[14] A. M. Abdulateef, "Evaluating the Thermal Performance of Steam Condenser Heat Exchanger in a Coal Fired Power Plant System," International Journal of Heat and Technology, vol. 41, no. 1, pp. 183–190, Feb. 2023, doi: 10.18280/ijht.410119.

[15] R. Laskowski, "A mathematical model of the steam turbine condenser for thermal power plant simulation," Applied Thermal Engineering, vol. 31, no. 14–15, pp. 2221–2228, Oct. 2011, doi: 10.1016/j.applthermaleng.2011.03.018.

[16] S. P. Lee and K. H. Kim, "Dynamic modeling of load-sharing steam headers in multi-unit industrial power plants," *Energy*, vol. 242, p. 122980, Mar. 2022.

[17] S. C. Kaushik, V. Siva Reddy, and S. Tyagi, "Energy and exergy analyses of thermal power plants: A review," Renewable and Sustainable Energy Reviews, vol. 15, no. 4, pp. 1857–1872, May 2011, doi: 10.1016/j.rser.2010.12.007.

[18] W. P. Utama and Y. S. Indartono, "Diagnostic evaluation of cooling water bio-fouling and seasonal sea temperature variation on steam condenser vacuum," *Journal of Applied Research and Technology*, vol. 21, no. 2, pp. 180–191, Apr. 2023.

[19] S. H. Ali, A. T. Baheta, and S. Hassan, "Effect of low pressure end conditions on steam power plant performance," MATEC Web of Conferences, vol. 13, p. 02010, 2014, doi: 10.1051/matecconf/20141302010.

[20] IAPWS, *Revised Release on the IAPWS Formulation 1997 for the Thermodynamic Properties of Water and Steam (IAPWS-IF97)*, International Association for the Properties of Water and Steam, Doorwerth, The Netherlands, 2014.

NOMENCLATURE

M_s : Main steam mass flow rate (kg/s or T/h)
P_1 : Turbine inlet steam pressure (MPa)
T_1 : Turbine inlet steam temperature (˚C)
T_2 : Turbine exhaust steam temperature (˚C)
$P_{cond,abs}$: Condenser absolute pressure (kPa)
P_{vac} : Condenser vacuum pressure (kPa)
h_1 : Specific enthalpy of inlet superheated steam (kJ/kg)
h_2 : Actual specific enthalpy of exhaust steam (kJ/kg)
h_{2s} : Isentropic specific enthalpy of exhaust steam (kJ/kg)
h_f : Specific enthalpy of saturated liquid (kJ/kg)
h_g : Specific enthalpy of saturated vapor (kJ/kg)
s_1, s_2 : Specific entropy of steam (kJ/(kg · K))
x_{2s} : Steam dryness quality fraction (dimensionless)
W_t : Internal mechanical turbine power (MW)
W_{gen} : Generator electrical power output (MW)
η_t : Turbine isentropic efficiency (%)
η_{conv} : Overall turbine-to-generator conversion ratio (%).

AUTHOR(S) BIOGRAPHY

Frendy Anwar Simangunsong
received his Bachelor of Applied Science (S.Tr.T) degree in Energy Generation Engineering Technology from Politeknik Negeri Batam, Indonesia, in 2026. His research interests include thermal power plant optimization, thermodynamic modeling, and heat exchanger performance evaluation.

Ir. Fauzun Atabiq, S.T., M.Cs
is a lecturer and researcher in the Department of Electrical Engineering at Politeknik Negeri Batam. His research focuses on energy conversion systems, power plant engineering, and industrial process control.

 https://doi.org/10.25077/xxxxx